

## SUPPLEMENTAL FIGURE LEGENDS

**Figure S1:** Association of Nr4a1 knockout mutation with proteinuria by linkage analysis. **(A)** Location of Nr4a1 mutation in exon 1 induced by ENU mutagenesis. The point mutation results in a stop codon [TAC (Tyrosine) to TAA (stop)]. **(B)** AseI restriction site polymorphism was used to perform linkage analysis in an F<sub>2</sub> (FHH x Nr4a1<sup>-/-</sup>) population (n=175). **(C)** Association of Nr4a1 mutation (A/A) with increased proteinuria (week 8 and 12), and reduced body weight (BW) and increased kidney weight (KW) at week 12 compared to wild-type (C/C). \* p<0.05 (week 8); † p<0.05 (week 12); mean values + SE are presented.

**Figure S2:** Autoregulation of renal blood flow (RBF) in FHH and Nr4a1<sup>-/-</sup> rats. **(A)** RBF was measured as renal perfusion pressure (RPP) was varied from 150 to 90 mmHg in steps of 10 mmHg. The dashed line represents an autoregulation curve that demonstrates perfect autoregulation. **(B)** Autoregulatory index (AI) was calculated over the range of pressures from 100 to 140 mmHg. AI of 0 indicates perfect autoregulation of RBF and AI of 1 is characteristic of a circulation with a fixed vascular resistance and impaired RBF autoregulation. FHH (as expected) and Nr4a1<sup>-/-</sup> rats demonstrate impaired regulation of RBF.

**Figure S3:** Serum lipid levels and hepatic steatosis in FHH and Nr4a1<sup>-/-</sup> rats at week 24. **(A)** Serum cholesterol and triglyceride levels. **(B)** H&E and Oil Red O staining in liver sections. \*p<0.05 vs. FHH; mean values + SE are presented.

**Figure S4:** Representative electron microscopy images of FHH and Nr4a1<sup>-/-</sup> kidney at week 24. **(A)** Image of glomerular capillary and podocyte foot processes. Thin arrows denote podocyte

foot process effacement. **(B)** Proximal tubule images. **(C)** Semi-quantitative assessment of cell degeneration (e.g., evidence of cells that are falling apart, loss of organelles, etc.) and lipid accumulation from electron microscopy images [n=15-20 tubule images per group (n=4 each strain)]. Each parameter was scored in blinded fashion on semi-quantitative scale of 0 (no evidence) to 3 (severe). Thick arrows denote lipid droplet in proximal tubule. \*p<0.05 vs. FHH; mean values + SE are presented.

**Figure S5:** Measurement of tubular injury in FHH and Nr4a1<sup>-/-</sup> rats at week 8, 16, and 24. **(A)** Semi-quantitative analysis of tubular injury. Tubular injury was analyzed for degree of tubular atrophy, vacuolization, dilation, and proteinaceous casts on a scale from 0 (normal) to 4 (severe with > 75% tubules demonstrating injury). **(B)** Quantitative real-time PCR of macrophage markers (Cd-68 and Socs3) and tubular injury genes [kidney injury molecule (Kim-1), and Neutrophil gelatinase-associated lipocalin (Ngal)]. n=20 images per group (n=6); \* p<0.05 compared to FHH; mean values + SE are presented.

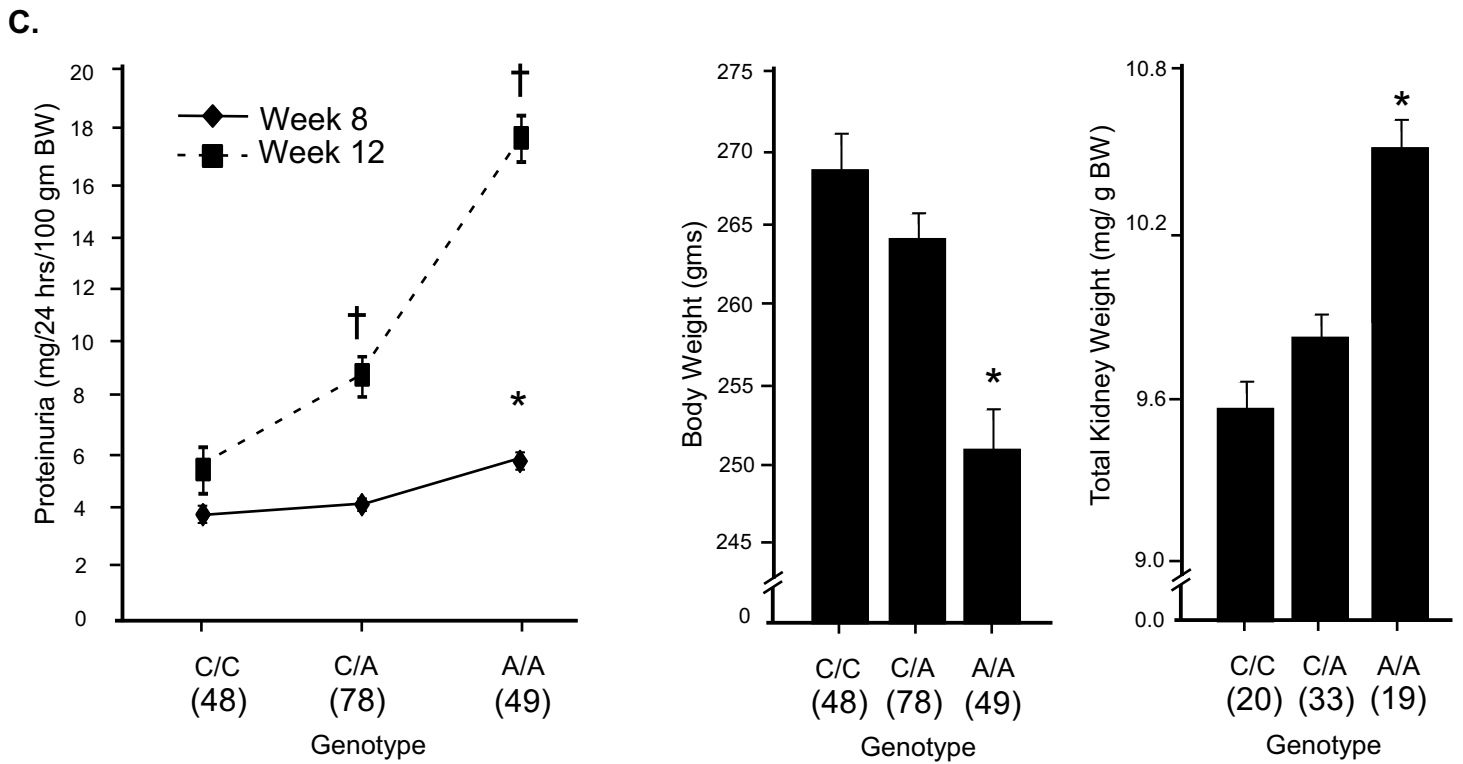
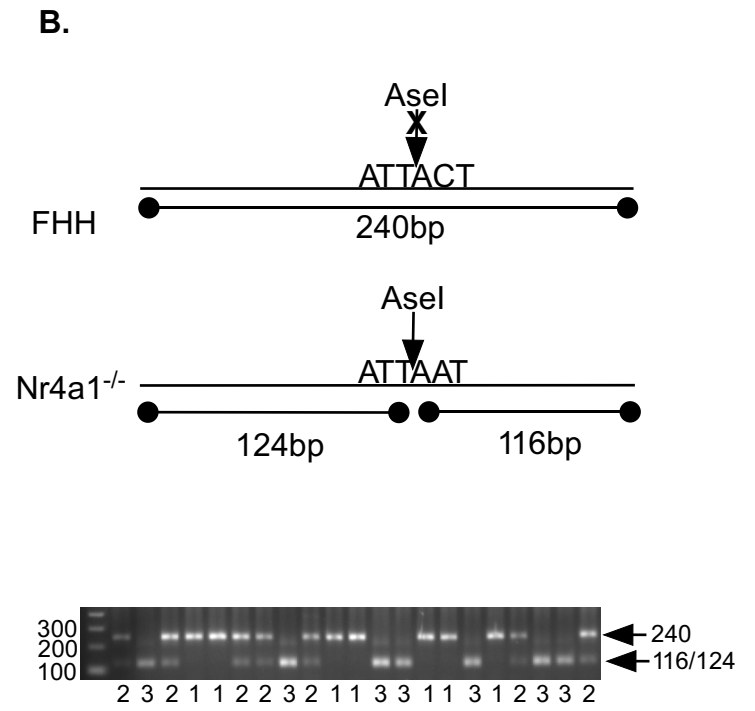
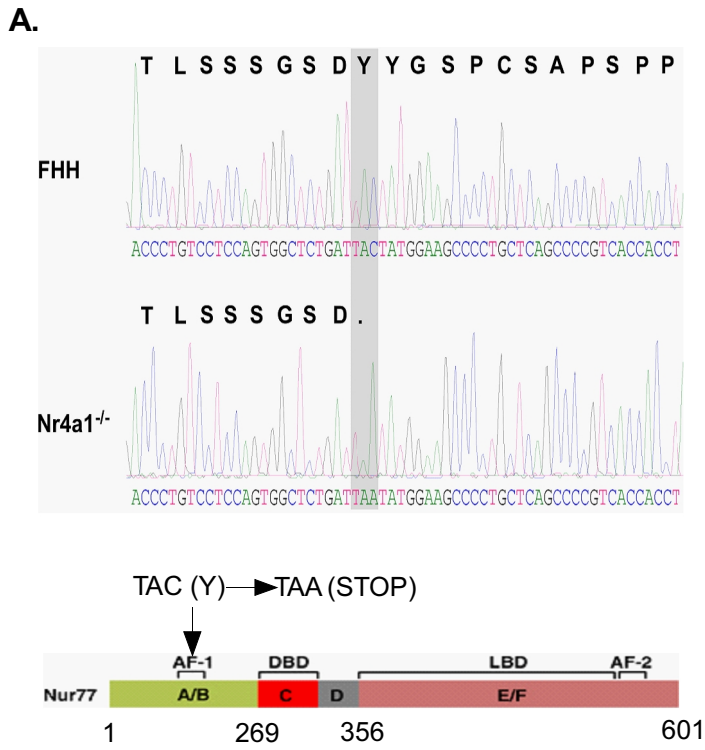
**Figure S6:** Microarray analysis of kidney cortex from FHH and Nr4a1<sup>-/-</sup> at week 8, 16, and 24. **(A)** Hierarchical clustering of immune related genes depicting gene expression changes with time and between the FHH and Nr4a1<sup>-/-</sup> strains. **(B)** Principal component analysis (PCA) illustrating the relationship between sample groups and gene expression changes over time. At an early time point (week 8) gene expression patterns are similar in kidney from Nr4a1<sup>-/-</sup> and FHH. From week 8 to week 16-24, gene expression differences of Nr4a1<sup>-/-</sup> are distinct from FHH and each other. By week 16, FHH gene expression differences are distinct from week 8, but similar to week 24. **(C)** Top biological functions (Ingenuity Pathway Analysis) and upstream regulators

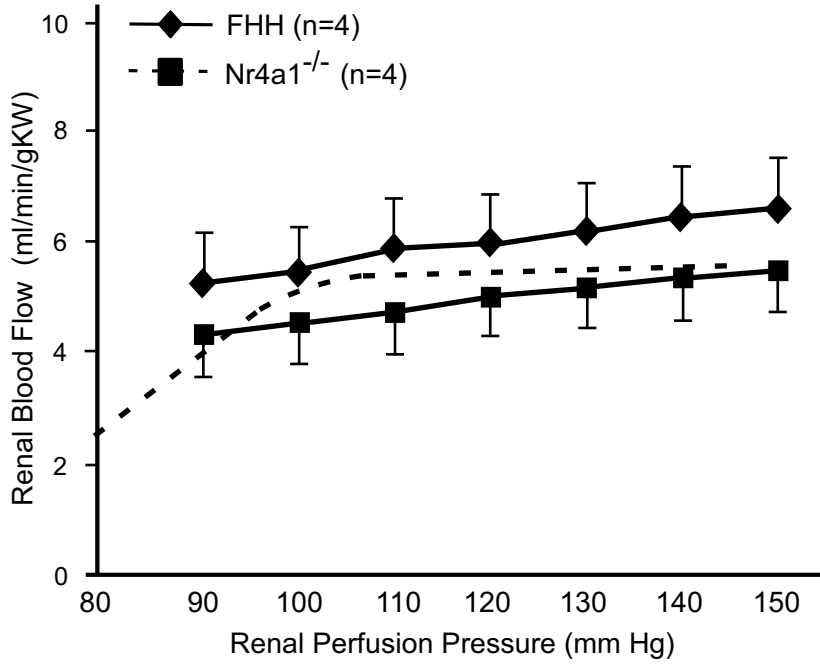
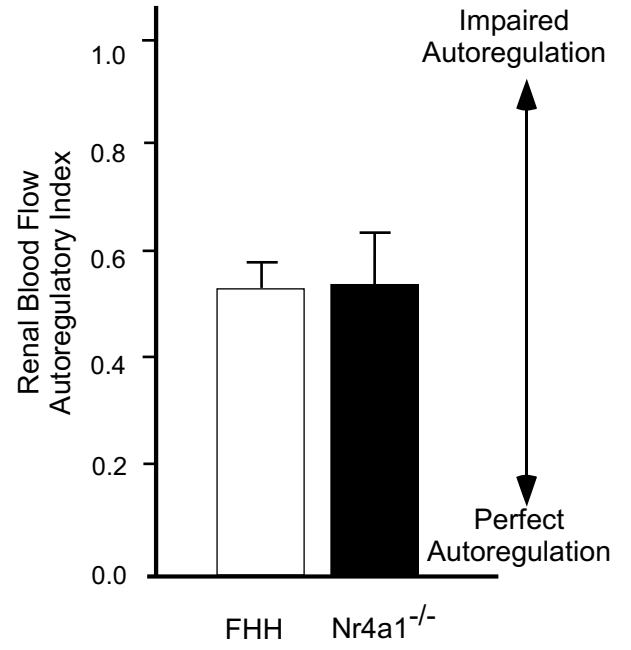
associated with gene expression difference (between samples and with time). **(D)** Quantitative real-time PCR validation of important chemokines/cytokines identified as differentially expressed between Nr4a1<sup>-/-</sup> and FHH.

**Figure S7:** Genotype, metabolic and renal injury measurements for bone marrow cross-transplantation studies using FHH and Nr4a1<sup>-/-</sup>. **(A)** Validation that bone marrow transplanted from FHH was successfully transplanted into Nr4a1<sup>-/-</sup> (FHH<sub>bm</sub> into Nr4a1<sup>-/-</sup><sub>irr</sub>) by PCR. All FHH<sub>bm</sub> into Nr4a1<sup>-/-</sup><sub>irr</sub> animals exhibited a heterozygous genotype (i.e., FHH and Nr4a1), whereas each parental control demonstrated homozygous genotype. **(B)** Serum cholesterol and triglyceride levels. **(C)** Semi-quantitative analysis of tubular injury [n=20 images per group (n=6-8)]. \* p<0.05 compared to FHH; mean values + SE are presented. † p<0.05 vs. other groups.

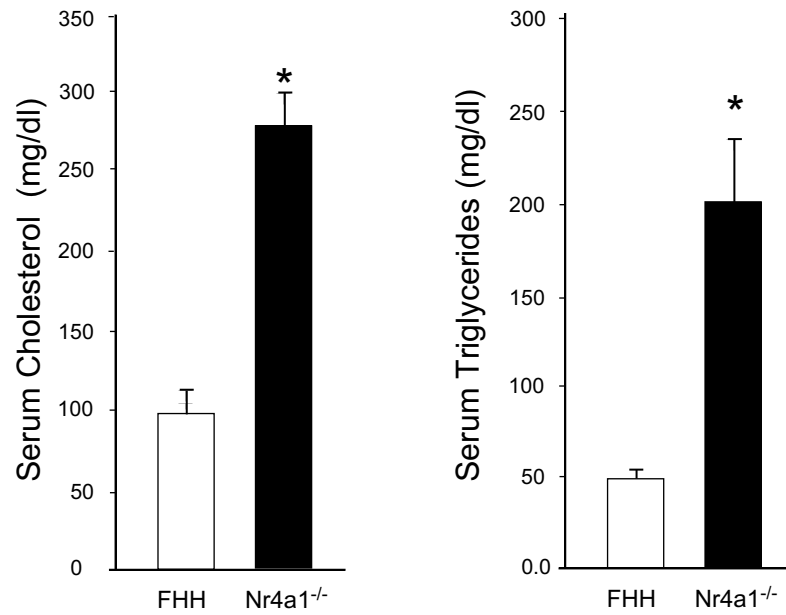
**Figure S8:** Quantitative real-time PCR of important inflammatory genes in thioglycolate elicited macrophages (**Fig. 4**) and bone-marrow derived macrophages. **(A)** Thioglycolate elicited macrophages isolated from Nr4a1<sup>-/-</sup> at week 4, 8, 12, and 20 under baseline conditions (unstimulated) demonstrated down-regulation (compared to FHH macrophages) of Il10, Il12b, and Tnfa and up-regulation of Nos2 from week 4-8, but by week 12 or 20 only Nos2 was significantly changed (increased in Nr4a1<sup>-/-</sup>). Kruppel-like factor 4 (Klf4) was significantly down-regulated and suppressor of cytokine signaling 3 (Socs3) was up-regulated, along with increased Nos2 expression suggest that macrophage isolated from Nr4a1<sup>-/-</sup> are primed toward M1 polarized pro-inflammatory phenotype. **(B)** Quantitative real-time PCR of inflammatory genes using bone marrow derived macrophage (n=6 independent cell cultures/treatment derived from

n=2 rats/group) from untreated and LPS treated macrophages from FHH and Nr4a1<sup>-/-</sup>. Bone marrow Nr4a1<sup>-/-</sup> macrophages demonstrated a significant up-regulation of Il-6, Il-12b, Tnfa, and Nos2 compared to FHH macrophages after stimulation with LPS. ND; not detected. \* p<0.05 compared to FHH; mean values + SE are presented.

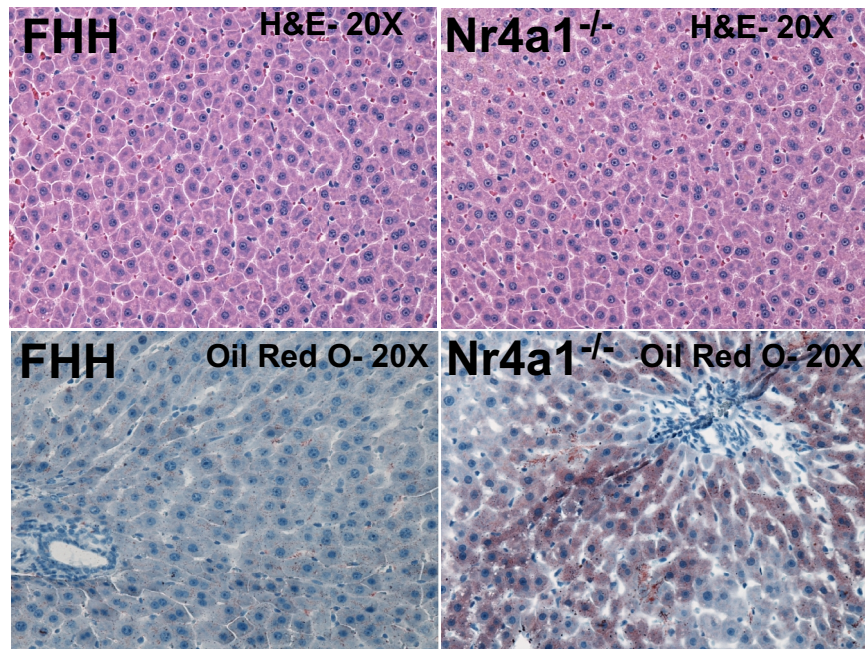


**A.****B.**

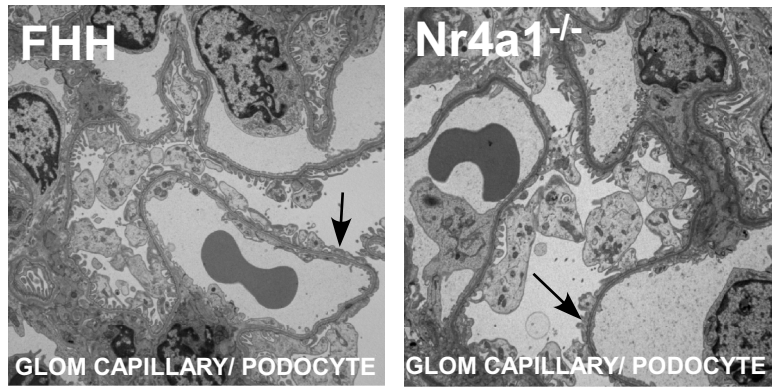
**A.**



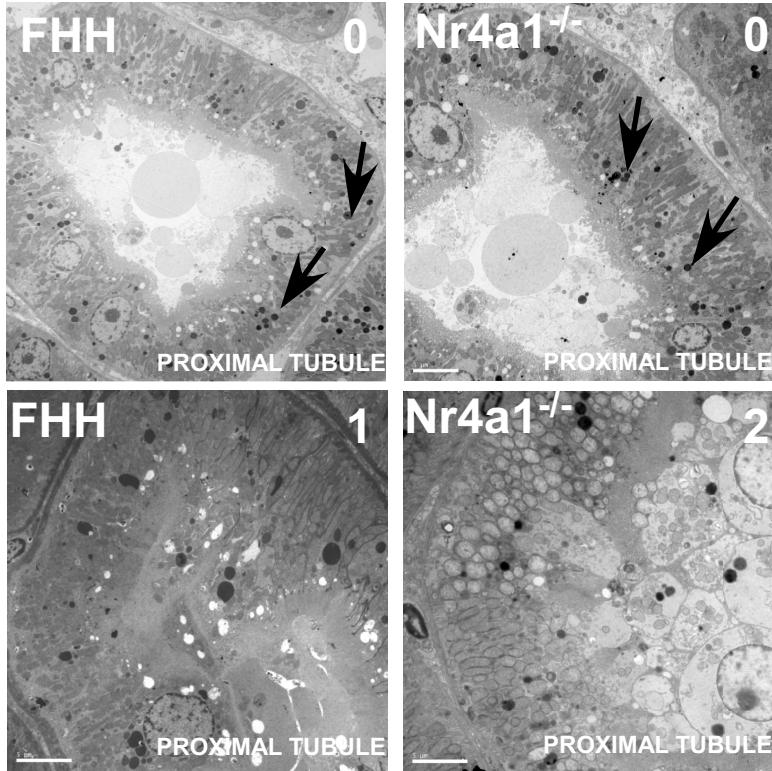
**B.**



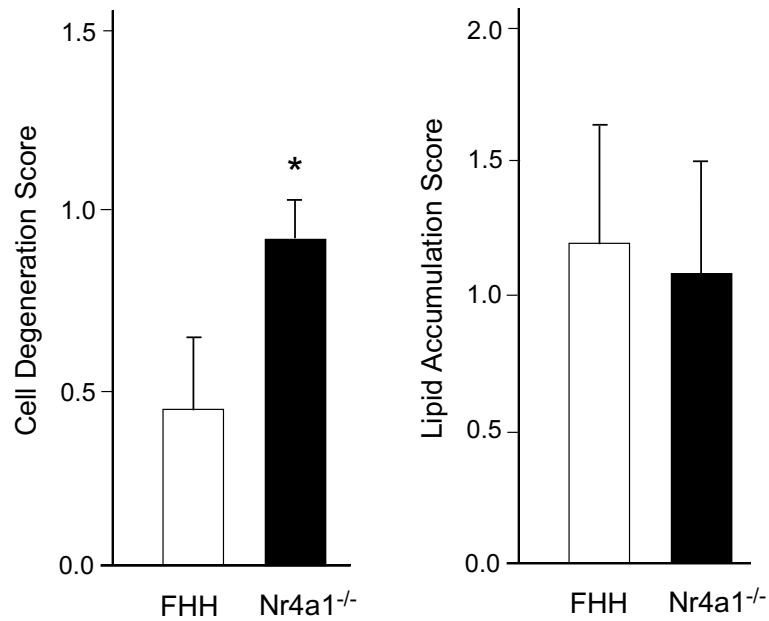
A.



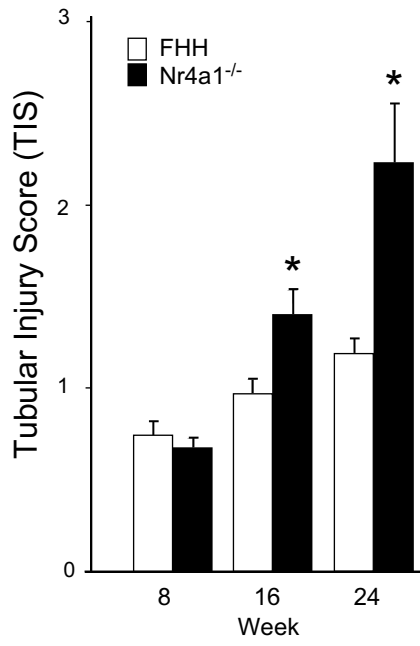
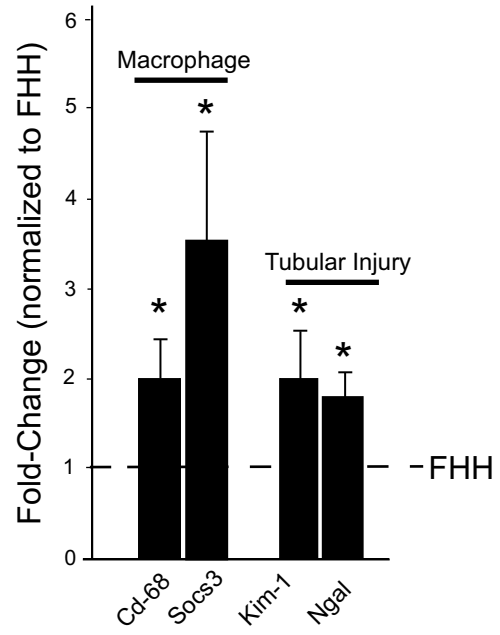
B.



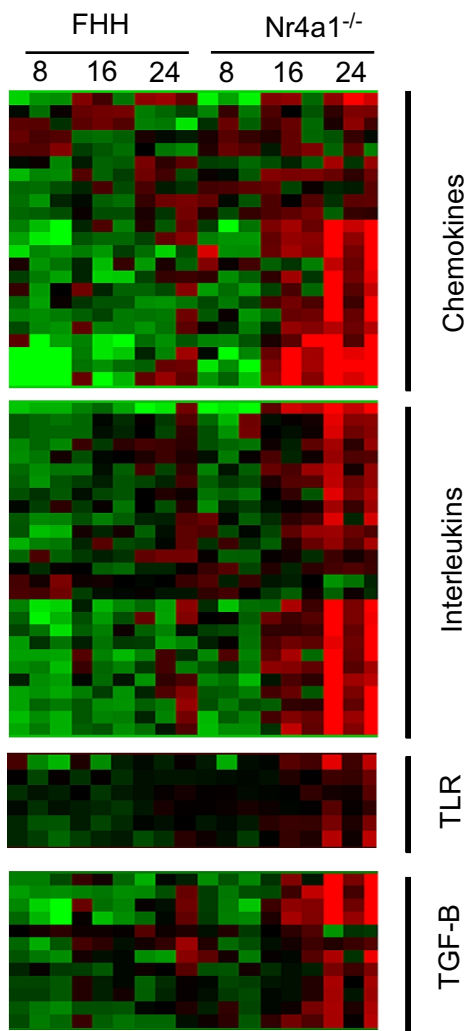
C.



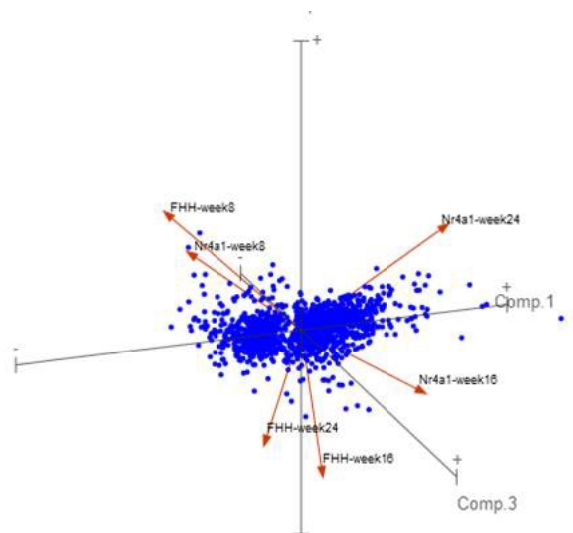


**A.****B.**

**A.**



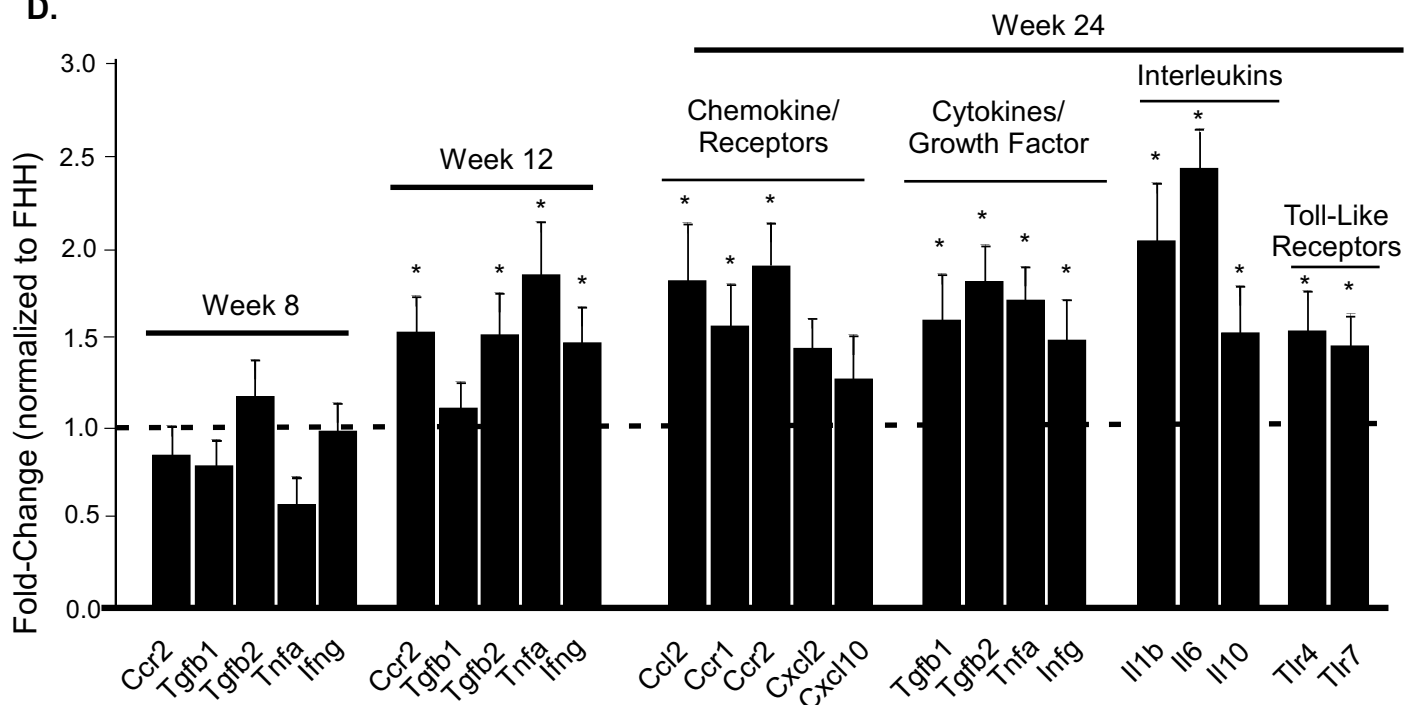
**B.**



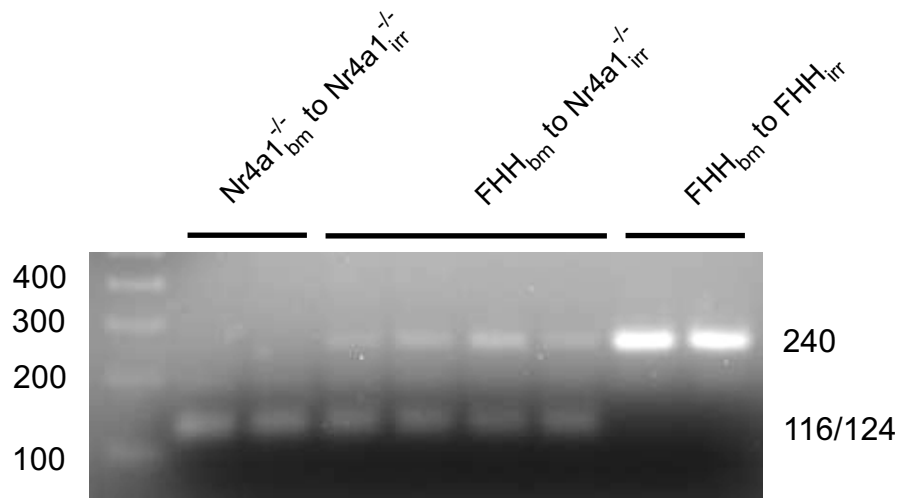
**C.**

Top Bio Functions		
<b>Diseases and Disorders</b>		
Name	p-value	# Molecules
Inflammatory Response	2.45E-14 - 3.15E-04	65
Connective Tissue Disorders	5.23E-12 - 1.47E-04	48
Inflammatory Disease	5.23E-12 - 2.50E-04	67
Skeletal and Muscular Disorders	5.23E-12 - 1.47E-04	47
Immunological Disease	8.85E-12 - 2.74E-04	54
<b>Upstream Regulator</b>		
	p-value of overlap	
lipopolysaccharide	3.11E-17	
IFNG (includes EG:15978)	6.42E-16	
IL1B	4.92E-12	
IL6	9.14E-12	
TNF	1.03E-11	

**D.**

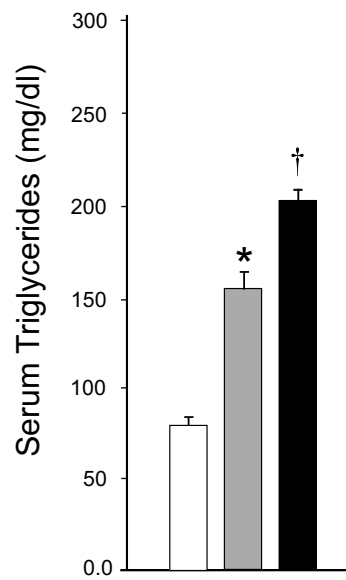
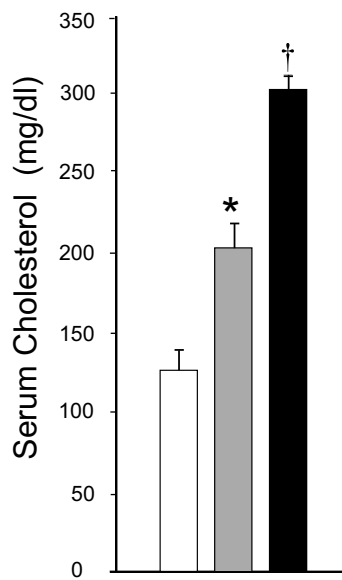


**A.**

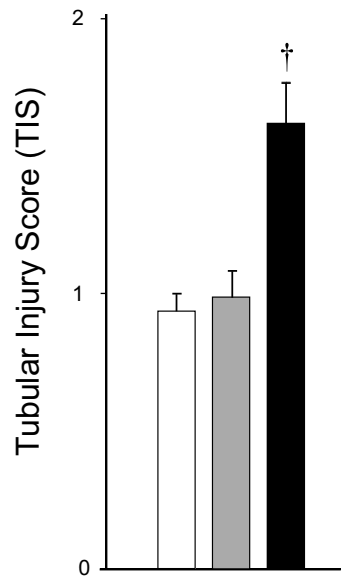


**B.**

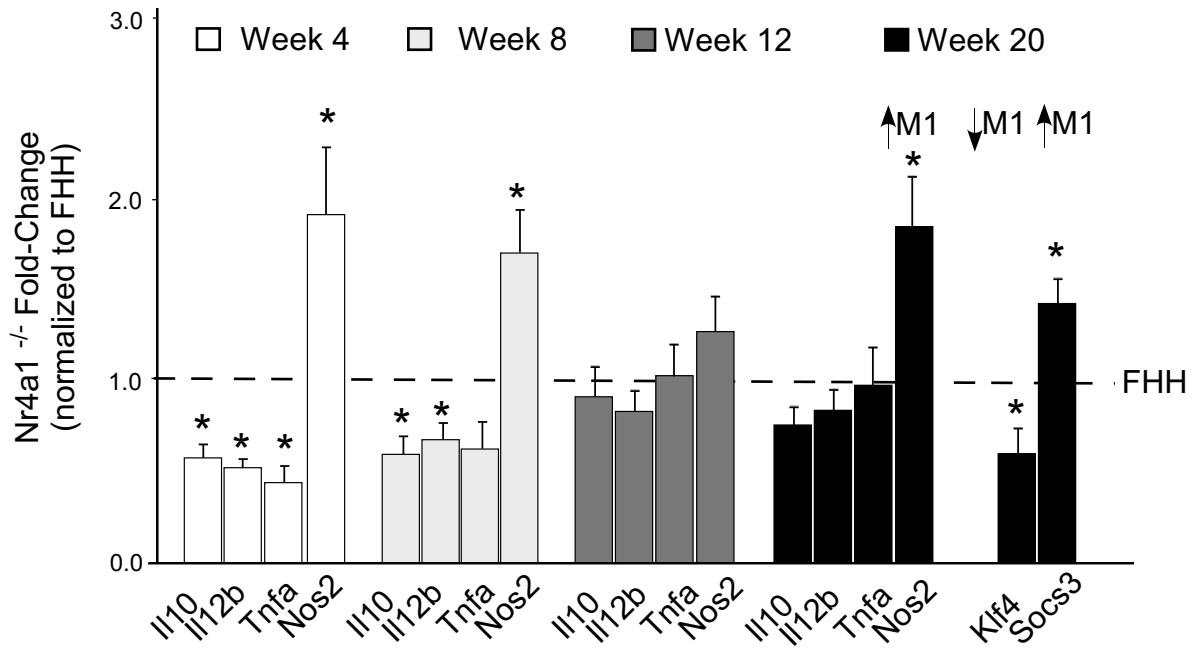
□  $FHH^{b/m}$  to  $FHH^{i/r}$     ■  $FHH^{b/m}$  to  $Nr4a1^{i/r}$     ■  $Nr4a1^{b/m}$  to  $Nr4a1^{i/r}$



**C.**



**A.**



**B.**

